Evaluation of mechanical, thermal and water absorption behaviors of *Polyalthia longifolia* seed reinforced vinyl ester composites

B. Stalin[1, *], N. Nagaprasad[2], V. Vignesh[3], M. Ravichandran[4], Nagarajan Rajini[5, *], Sikiru Oluwarotimi Ismail[6], Faruq Mohammad [7]

[1]Department of Mechanical Engineering, Anna University, Regional Campus Madurai, Madurai- 625 019, Tamil Nadu, India.

[2]Department of Mechanical Engineering, ULTRA College of Engineering and Technology, Madurai- 625107, Tamil Nadu, India.

[3]Department of Mechanical Engineering, Sethu Institute of Technology, Pulloor, Kariapatti – 626 115, Tamil Nadu, India.

[4]Department of Mechanical Engineering, K. Ramakrishnan College of Engineering, Samayapuram, Tiruchirappalli- 621 112, Tamil Nadu, India.

[5]Department of Mechanical Engineering, Kalasalingam University, Krishnankoil, Virudhunagar- 626 126, Tamil Nadu, India.

[6]Department of Engineering, Centre for Engineering Research, School of Engineering and Computer Science, University of Hertfordshire, Hatfield, AL10 9AB, England, UK.

[7] Department of Chemistry, College of Science, King Saud University, Riyadh, 11451, Kingdom of Saudi Arabia.

[*]Corresponding authors: N. Rajini, rajiniklu@gmail.com, +91-9942139392

B. Stalin, stalin1312@gmail.com, +91-9865264158

Abstract

This study presents a novel utilization of biomass solid waste, named *Polyalthia longifolia* (Mast tree) seed as a reinforcement in a composite, using a compression molding technique. An attempt was made to reinforce vinyl ester matrix (VE) with *Polyalthia longifolia* seed filler (PLSF), ranging from 5 to 50 wt% loadings. Mechanical properties of the fabricated *Polyalthia longifolia* seed filler/vinyl ester (PLSF-VE) composite samples were tested and analyzed. The results showed that the PLSF-VE composite exhibited optimum mechanical properties at 25 % wt of filler loading; ultimate tensile strength and modulus were approximately 32.50 MPa and 1.23 GPa, respectively. The ultimate flexural, impact strengths and hardness were observed around 125 MPa, 31.09 kJ/m^2 and 36.50, respectively. The heat deflection test and thermo-gravimetric analysis depicted that the PLSF-VE composites withstood up to 66 ^{o}C and 430 ^{o}C, respectively. Furthermore, the PLSF and its various composite samples were studied, using energy-dispersive X-ray (EDX), X-ray diffraction (XRD), Fourier transform infrared spectroscopy (FTIR) and scanning electron microscope (SEM).

Keywords: *Polyalthia longifolia* seed filler, Vinyl ester, Compression molding, Properties, Characterization.

1. Introduction

In recent years, using bio-fillers for development of biodegradable composite has received much attention, as they are environmentally friendly. Acceptably, polymers are reinforced with fibers or fillers to produce materials that are suitable for industrial requirements. *Polyalthia longifolia* tree is mostly used for manufacturing small articles, such as pencil boxes, lightweight trunk and various herbal preparations. The lightweight trunk was used earlier in making masts for sailing ships; therefore, its name becomes Mast tree. In a continuous effort to upgrade their values, the possible application of fillers from *Polyalthia*

longifolia seeds was explored. The rationale behind making an attempt to use this plant material include their natural renewability, biodegradability, sustainability as well as non-toxicity. Thus, it becomes an environmental friendly reinforcing material with respect to its harmless processing and disposal. The various influences of nutshells from pistachio, almond, walnut and pecan on polymer composites have been reported (Dixit, Mishra, Pal, Rana, & Upreti, 2014; Rao & Rehman, 2012; Sánchez-Acosta et al., 2019; Sutivisedsak et al., 2012).

Today environmentalists and researchers have strived hard to reduce the industrial wastes accumulated over the surface of the earth. Several researchers use industrial wastes to fabricate composite materials and reduce environmental pollution, caused by inexpensive hazardous material from industries. By using the non-toxic materials, accumulated waste substances on earth will be reduced. Therefore, living safely on earthly will be more supported (Richard et al., 2019; Vigneshwaran et al., 2019). In a particulate-filled polymer composite, the mechanical strength strictly depends on particle size, shape, dispersion of particle into the matrix of the composite and also fiber or particle-polymer matrix interfacial bonding (Richard et al., 2019). The mechanical behaviors of a polymer matrix have been enhanced by incorporating several industrial wastes, including fly ash, sewage sludge ash and silicon carbide micro-particles to the matrix used (Erkliğ, Alsaadi, & Bulut, 2016). Clay, as an organic filler, has also been added to polymer composites to improve the mechanical behaviors of the polymer composites, with a high specific surface area (Bensalah et al., 2017). Erdogan and Huner (2018) investigated the reinforcing influence of pinewood sawdust, black rice husk powder and walnut shell flour on polypropylene. A commonly used coupling agent, known as maleic anhydride polypropylene (MAPP) was used to study the strength of the composite. The results depicted that the mechanical behaviors of the composite decreased after adding the aforementioned reinforcements. However, adding MAPP increased both mechanical and physical behaviors of the biocomposites. Zheng, Sun, and Zhang (2019) prepared walnut shell

powder/poly (lactic acid) composites. Their results indicated that the maximum tensile strength obtained was 51.3 MPa; better mechanical strength up to 0.5 wt% of filler loading and then decreased because the walnut shell powder agglomerated more within the poly (lactic acid) matrix. Vaisakh et al. (2016) studied the micro and modified nano-size of SiO_2/Al_2O_3 reinforced epoxy composites. Their results showed that mixed-matrix SiO_2/Al_2O_3 ceramic filler matrix produced high compressive strength of 196 MPa and flexural modulus of 7.6 GPa. The nano-modified mixed-matrix SiO_2/Al_2O_3 showed a controlled rate of wear as well as reduction in friction coefficient. Various fillers of biochar particles derived from rice husk (Richard, Rajadurai, & Manikandan, 2016), fishbone (Abhishek et al., 2018), hemp hurds, alfalfa, and grape stem (Battegazzore, Noori, & Frache, 2019), lignocellulosic wood (Kumar, Kumar, & Bhowmik, 2018), thyme herbs (Montanes, Garcia-Sanoguera, Segui, Fenollar, & Boronat, 2018), rice husk ash and siliceous earth-Sillitin Z 86 (Pongdong, Kummerlöwe, Vennemann, Thitithammawong, & Nakason, 2018) have been added to various polymer matrices to reduce the materials (polymers) cost, enhance important properties of the resultant composites, such as mechanical, dimensional and thermal stability.

This work explored the possibility of using *Polyalthia longifolia* (Mast tree) seed powder as a reinforcement in vinyl ester resin for the development of partially biodegradable composite material. The mechanical behaviors, including tensile, impact, flexural as well as hardness of *Polyalthia longifolia* seed filler/vinyl ester (PLSF-VE) composite samples with various filler contents or loadings, ranging from 5 to 50 wt%) were analyzed. Stability of the various samples in four different aquatic environments was studied, using water absorption test. Finally, the fractured surface structures of PLSF-VE composites were observed, using a scanning electron microscopy (SEM) and other techniques in order to comprehend and establish the correlation between the surface structure and filler-matrix interfacial adhesion or strength of the composites. The contributions of this present study include, but are not limited

to, deeper understanding of various mechanical, thermal as well as water absorption behaviors of innovative PLSF-VE composites.

2. Experimentation and methodology

2.1 Materials

The Mast tree (*Polyalthia longifolia*, density of 0.49 g/cm^3) belongs to the Annonaceae family. It is found in India, Sri Lanka and many tropical countries around the world, as an ornamental street tree. In Indian subcontinent and adjacent areas, Mast tree is important in the cultural traditions. Because of the close resemblance of the Ashoka tree (*Saraca indica*), it is sometimes incorrectly identified as Ashoka tree. A 5 kg of *Polyalthia longifolia* seeds (PLS) were collected from Madurai, Tamil Nadu, India. The seed coats were removed from the seed manually, and it was purified with distilled water. After purification, seeds were dried in sunlight for 2 weeks. The dried PLS were crushed to a fine powder in a ball mill, before sieving the *Polyalthia longifolia* seed filler (PLSF) to obtain a mean size of 25-50 µm. The mean particle size of the milled PLSF was measured, using Horiba SZ-100 particle analyzer. The matrix used was an untreated vinyl ester resin, in addition to other chemicals: Bisphenol-A-epoxy vinyl ester resin (styrene-45%) and N-Dimethylaniline (accelerator). Both methyl ethyl ketone peroxide and cobalt naphthenate were used as a catalyst and promoter, respectively. These chemicals were supplied by the Covai Seenu Company, India (Stalin, Nagaprasad, Vignesh, & Ravichandran, 2019).

2.2 Manufacture of composites

A traditional compression molding method was adopted to prepare different PLSF-VE composite samples, with filler loadings of 5 – 50 wt%. Fig. 1 shows the various stages of preparation of PLSF. An untreated vinyl ester resin was poured into a container and initially stirred for 15 minutes to remove air bubbles, then a measured quantity of PLSF was added. To

start with, a 5 wt% of PLSF was added to the resin and stirred for 20 minutes. This was necessary to have a uniform mixture. The resin was mixed with accelerator, promoter and catalyst of 1.5 wt%, each according to the recommendation from the supplier. Later, it was slowly decanted into a wax-coated mold cavity size of 200 x 200 x 3 mm. After it has been fully discharged into the mold cavity, the upper die was closed and the compression took place under a pressure of 100 kPa. Better curing took place after 24 hours at a room temperature, as expected (Erkliğ et al., 2016; Vigneshwaran et al., 2019).

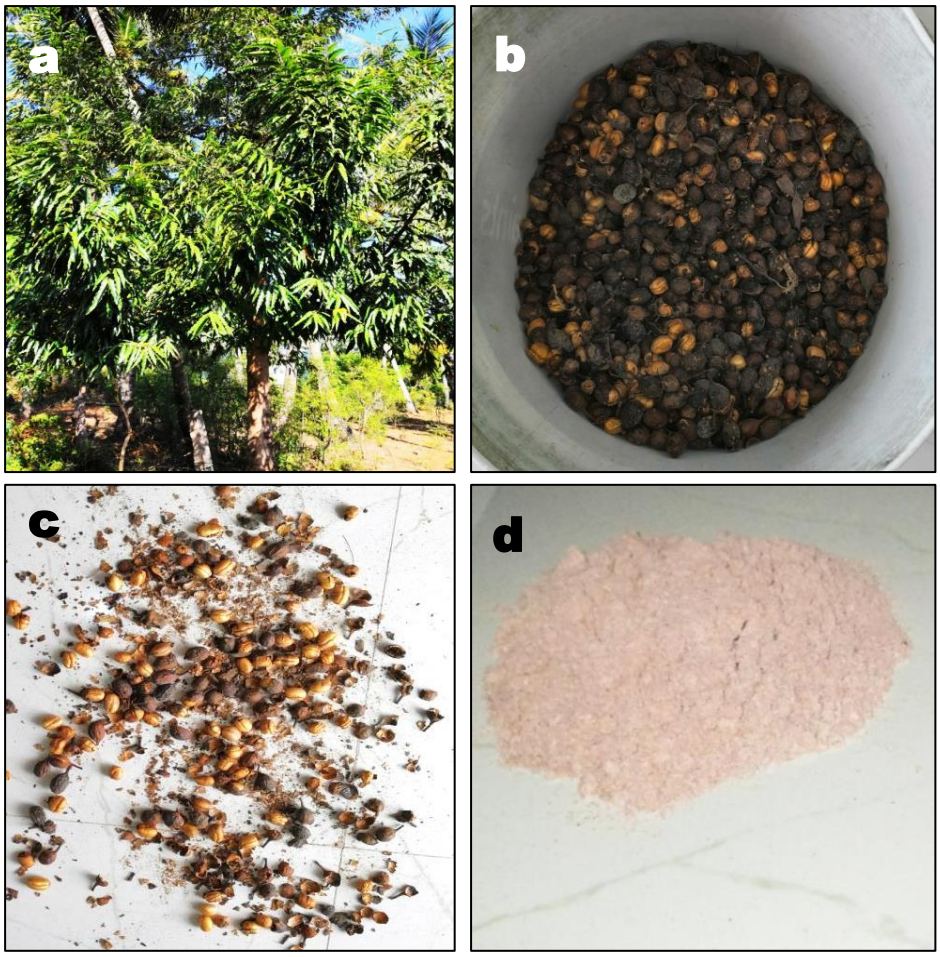

Fig. 1. Preparation of *Polyalthia longifolia* seed powder: *Polyalthia longifolia* (a) tree, (b) seed, (c) seed extraction, and (d) seed powder.

2.3 Characterization methods

2.3.1 Physico-chemical properties

Chemical composition analysis was used to determine the percentage of cellulose, lignin, wax, moisture, and ash content present in *Polyalthia longifolia* seed powder. The chemical composition of the *Polyalthia longifolia* seed powder was determined, using the following test methods: Cellulose: Kurschner and Hoffer's method (Mayandi et al., 2015), lignin: Klason method (Mayandi et al., 2015), wax: Conrad method (Conrad, 1944), ash: According to the ASTM E1755-61 standard (Mayandi et al., 2015), and density: Mettler Toledo xsz05 balance method (Sathishkumar, Navaneethakrishnan, & Shankar, 2012). The samples were dried in an oven at 104 °C for 4 hours (Mayandi et al., 2015) to determine the moisture content. For all the analyses carried out, three samples were taken and the average of three samples with standard deviation values were reported.

2.3.2 X-ray diffraction

An X'Pert-Pro diffractometer system was used to perform the X-ray diffraction (XRD) analysis of the PLSF. To obtain information about the dimensions of unit cells as well as crystalline material phase identification, a rapid analytical technique was employed. A continuous scan mode of the powder specimens was carried to obtain 2θ data, from 10° to 80°, using a monochromatic Cu–Kα radiation wavelength of 0.154 nm. From Eq. (1), the PLSF crystallinity index (*CI*) was evaluated.

$$CI = \frac{IC - Iam}{IC} \, x \, 100 \qquad (1)$$

Where *IC* represents maximum intensity of the peak (2, 0, 0). This quantity corresponds to the crystalline fraction and I_{am} denotes minimum intensity of the peak (1, 1, 0). It quantifies the amorphous fraction. Also, From Eq. (2); Scherer's formula was used to determine the crystallite size (CS) of the intermolecular forces (IMFs) for the crystallographic plane (2, 0, 0).

$$CS = \frac{K\lambda}{\beta cos\theta} \quad (2)$$

Where k = Scherer constant (usually 0.84), λ = X-ray wavelength of 0.154 nm, b = peak's full width occurred at half-maximum, and h = Bragg angle (Vignesh, Balaji, Karthikeyan, 2016; Nagarajan et al., 2020).

2.3.3 Fourier transform infrared spectroscopy

By using Fourier transform infrared spectroscopy (FTIR), PLSF molecular structure was analyzed, using a Perkin Elmer Spectrum RXI FTIR spectrometer in a KBr matrix. The recording of the spectra took place at wave number ranged from 400 to 4000 cm^{-1}, scan rate and resolution of 32 scans/minute and 2 cm^{-1}, respectively. KBr was mixed with the *Polyalthia longifolia* seed powder. Then, the pellet forms were prepared through the pressurization method to obtain the FTIR spectra of the specimen in a standard condition (Kumar et al., 2018; Vignesh et al., 2016).

2.4 Mechanical tests

The tensile strengths of the various samples were evaluated, using Tinius OlsenH50K. The test crosshead speed of the tensile testing machine was 1 mm/min. Five specimen replicates, with the dimension of 165×10×3 mm each, were taken for each weight percentage in accordance with ASTM D638 standard (Stalin et al., 2019). The mechanical tests on flexural strengths of all the various samples (neat vinyl ester and its PLSF-VE composites) were performed at a room temperature, according to ASTM D790-10 standard (127 x 12.7 x 3 mm), using a digital universal testing machine (Vignesh, Balaji, & Karthikeyan, 2017). In addition, for this same study, the impact strengths of the same various specimens were studied in agreement with ASTM D 256 standard (65 x 13 x 3 mm) at a room temperature, using a Charpy pendulum impact tester. Following the ASTM 2583 standard (Stalin et al., 2019), Barcol

hardness tester (Model: VBH2) was used to determine the hardness properties of the same various samples (Karthikeyan et al., 2016). In all the cases of mechanical properties, a single sample T-test was performed with the confidence interval of 95% to analyze the variation between the sample.

2.5 Microstructural examination

A JOEL SEM was employed to analyze the ruptured surfaces of the samples after tensile, flexural as well as impact tests, using scanning acceleration voltage ranged from 10 to 30 kV. A thin golden layer coating was done on surfaces of the fractured samples in a vacuum chamber with aid of a sputter coater before the non-destructive examination was performed. This was necessary to aid conductivity and produce clear micrographs.

2.6 Thermal studies

2.6.1 Heat deflection temperature test

A HDT-TSP model tester was used to conduct the heat deflection temperature (HDT) test in accordance with ASTM D648 standard (60 × 12 mm × 3 mm) for 0 – 50 wt% PLS filler loading composites. The loading pressure and uniform heating rate were 455 kPa and 2±0.2 °C/min, respectively. The HDT was noted when the test bar deflected; a standard deflection under flexural load.

2.6.2 Thermo-gravimetric and differential thermal analyses

The rate of change in the amount and weight of the samples were evaluated, using ModelSTA449 F3, Netzsch, Germany, during both thermo-gravimetric analysis (TGA) and differential thermal analysis (DTA). These quantities were obtained in a controlled environment and depended on either temperature or time. For all the composites, 10 milligrams of powder samples of PLSF-VE composites were put in a precision-balanced alumina crucible.

When determining the thermal stability of the composite samples, the temperature gradually increased to 1000 ^{o}C from a room temperature, with a heating rate within a nitrogen atmosphere and flow rate of 10 ^{o}C/min and 20 mL/min, respectively (Stalin et al., 2019; Pillai, Manimaran, & Vignesh, 2020).

2.7 Water absorption behavior

A minimum of three rectangular samples from each filler loading were produced from the fabricated sample plates with a dimension of 39 mm ×10 mm × 3 mm, in agreement with ASTM D570-99 standard. An oven was used to dry the specimens for 24 hours (a day) at a temperature tolerance of 102 ± 3 ^{o}C. Afterwards, specimens were exposed to the selected four different aqueous environments, which were normal, salt, hot and cold water, separately. The weight of the specimens before soaked in water was measured using an electronic balance, with an accuracy up to 10^{-4} g. Then, the specimens were soaked in normal, salt, hot and cold water at a room temperature for 24 hours, separately. A blotting paper was used to wipe off or clean water droplets on the surfaces of all the samples after they have been removed from the water, prior to each measurement.

Using Eq. (3), the absorbed moisture content of each of the samples was estimated.

$$M(t) = 100\,\frac{(Wt - Wo)}{Wo} \qquad (3)$$

Where W_t represents the specimen weight at a specified immersion time and W_o denotes the oven-dried weight (Akil, Cheng, Ishak, Bakar, & Rahman, 2009; Najafi, Kiaefar, Hamidina, & Tajvidi, 2007).

3. Results and discussion

3.1 Elemental studies

A JEOL-JSM-5610LV model was employed to examine the chemical constituents of the PLSF, during X-ray analysis. Fig. 2(a) depicts the results obtained. It was observed from

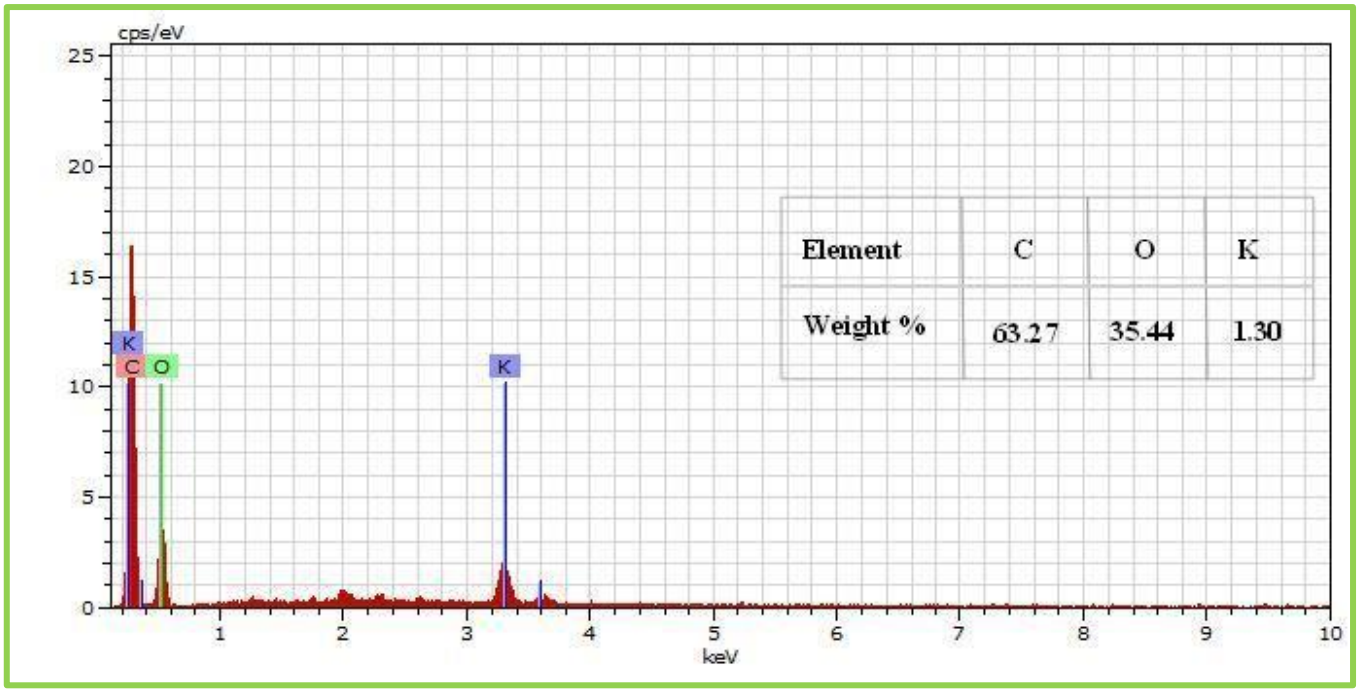

Fig. 2(a). SEM EDAX image of *Polyalthia longifolia* seed filler.

the results that the major components of PLSF included 63.27%, 35.44% and 1.3% of carbon, oxygen and potassium, respectively.

3.1.1 Physico-chemical properties

The material has a low density of 0.49 g/cm^3. From the chemical analysis, the cellulose content present in PLSF was 61.75%, which was higher than that of palm kernel shell, coconut sheath, rice husk, oil palm shell, groundnut shell, coconut shell and palm tree leaflet of 26.65, 27.00, 31.30, 32.60, 35.70, 36.30 and 40.21, respectively. In general, the mechanical strength of the composite mainly depended on the cellulose content present in the filler/fiber. The lignin content of 19.72% present in the PLSF produced protection against a biological attack. This content was greater than that of pulp fiber, rice husk and red coconut empty fruit bunch of 12.00, 14.30 and 15.82%, respectively (Nagarajan & Balaji, 2016). The wax, ash and moisture contents present in the PLSF were 0.52, 3.68 and 8.32%, respectively.

3.1.2 X-ray diffraction

X-ray diffraction analysis of the PLSF was conducted, as shown in Fig. 2(b). It presents two major crystalline peaks. The first peak estimated at 15.92° was attributed to low-intensity peak (110), which indicated an amorphous fraction (I_{am}). This was attributed to the fact that the filler contained an amorphous material; not a crystal. The second peak estimated at 22.51° was traced to high-intensity peak (200), which indicated the crystalline fraction (I_C). Therefore, the *CI* of PLSF was obtained at 65.57%. The *CI* of PLSF was greater than that of *Carexmeyeriana*, coconut empty fruit bunch, *Prosopis julifora*, Kusha grass, *Sanseveria cylindrica*, sisal and jute fibers (Balaji, Karthikeyan, & Vignesh, 2016; Vignesh et al., 2016). The PLSF crystallite size (L) was determined, using Scherer's formula; Eq. (2). The value peak's full-width at half-maximum (β) for PLSF was determined at 0.0293 rad. Furthermore, the angle of diffraction of X-rays within a crystalline material, known as the Bragg angle (θ) was determined to be 0.196. The calculated value of L for PLSF was 4.44 nm, using Scherer's equation, which indicated the moisture absorption and chemical reactivity resistance capacities of the PLSF. The 4.44 nm calculated value of L impacted the chemical reactivity and decreased the water absorption capacity behaviors of the PLSF material (Sreenivasan, Somasundaram, Ravindran, Manikandan, & Narayanasamy, 2011).

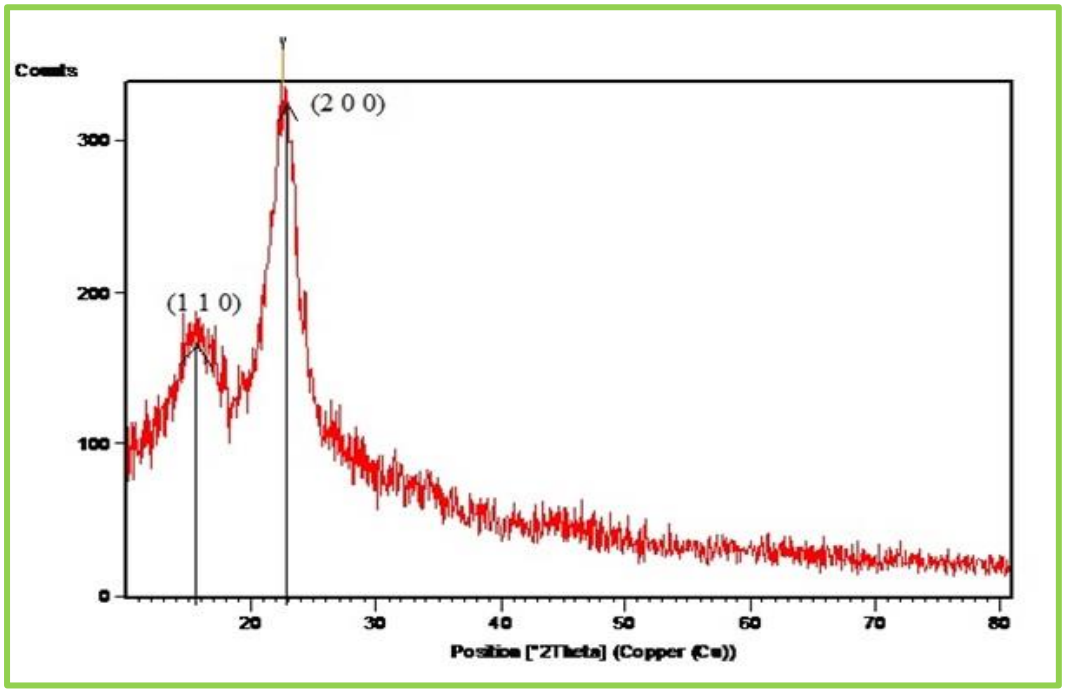

Fig. 2(b). XRD image of *Polyalthia longifolia* seed filler.

3.1.3 Fourier transform infrared spectroscopy

The results obtained from the FTIR spectroscopy of the PLSF are presented in Fig. 2(c), including the classical peaks. The spectra influenced the sharp peaks at 3850, 3417.84, 2924, 1731, 1644, 1382, 1251, 1046 and 584 cm^{-1} with reduced wave numbers. There were absorption bands of various cellulosic, lignin, hemicellulosic and wax chemical functional groups, exhibited by these compounds. The peaks at around 3417-3850 cm^{-1} can be traced to the presence of the hydrogen bond and alcohol group (O-H) as well as the stretching vibration of the cellulose molecules of -OH groups. Additionally, the peaks at 2356 cm^{-1} referred to CH_2 symmetrical stretching, due to the presence of wax (Sathishkumar, Navaneethakrishnan, & Shankar, 2012).

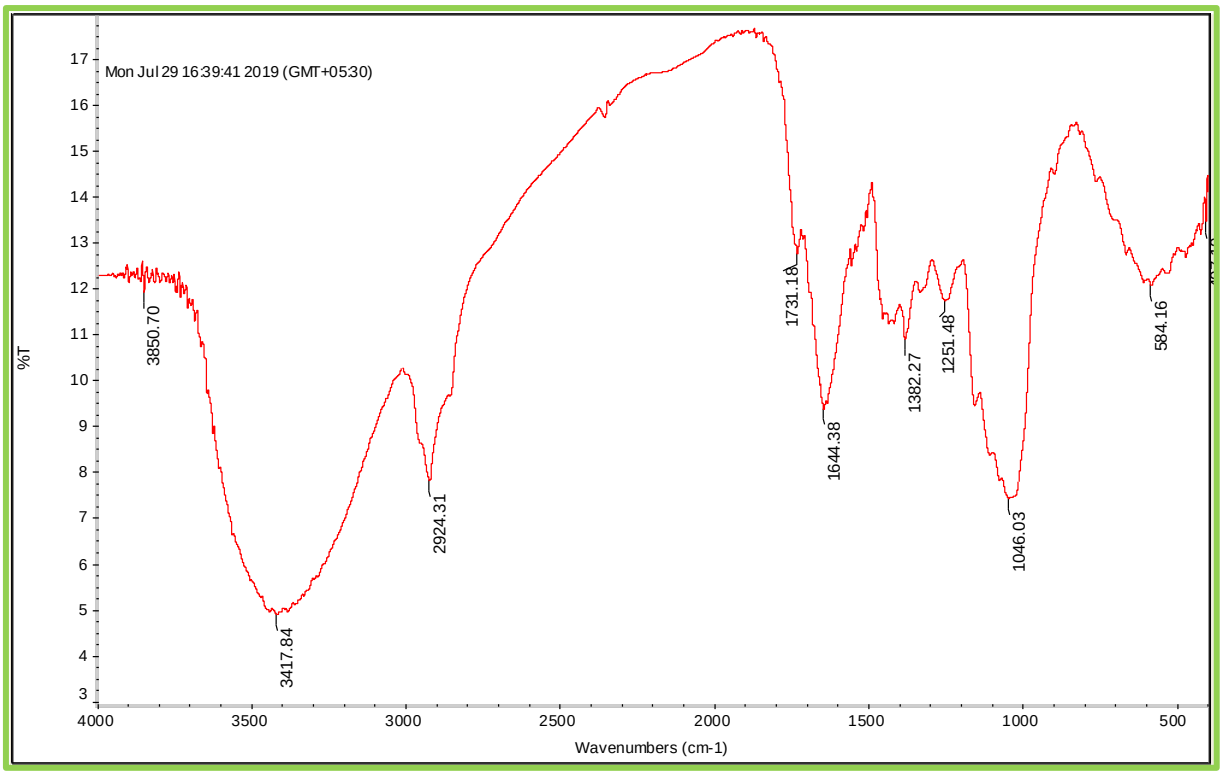

Fig. 2(c). FTIR image of *Polyalthia longifolia* seed filler.

The stretching vibration of carboxylic acid (RCOOH) and carbonyl (C=0) groups were obtained at 1731 cm^{-1}. The carbonyl group is present in ester (RCOOR'), while carboxylic acid

can be found in both lignin and hemicelluloses. There was a presence of absorbed water at the peak of 1644 cm^{-1}. Hence, this further confirmed the hydrophilicity of the PLSF. The peak value of 1251.48 cm^{-1} confirmed the C-O stretch of the -$COCH_3$ (acetyl) group, present in lignin materials. Due to the out-of-plane bending of OH, a broad band at 584.16 cm^{-1} was obtained (Gopinath, Ganesan, Saravanakumar, & Poopathi, 2016).

3.2 Mechanical behaviors

3.2.1 Tensile strength

A universal testing machine (UTM) was employed to obtain the tensile properties of the various samples. The tensile test was conducted until the tensile specimens were broken. Fig. 3(a) depicts the tensile strengths and moduli obtained from the various samples. The tensile strengths obtained from the PLSF-VE samples increased from 10 to 32 MPa with an increase in the filler contents; from 5 to 50 wt%. The strength increased from 24 to 26 MPa, when the filler content was increased from 0 to 5 wt%. The percentage of improvement after addition of filler was 7.69%. For 10 wt% filler content, the strength of PLSF-VE composite was slightly decreased, when compared with 5 wt%. This can be attributed to unevenly distribution between the filler and matrix. Moreover, the tensile strength of the PLSF-VE composites increased from 20 to 30 MPa, when the filler content increased from 10 to 20 wt%. The percentage of improvement between these fillers was 33%. Significantly, the ultimate tensile strength and modulus of PLSF-VE composites exhibited 32 MPa and 1.23 GPa at a higher PLSF weight content of 25 wt%, because of the higher load transfer from the filler to the vinyl ester matrix. However, the tensile strength of PLSF-VE composites decreased up to 10 MPa, when the filler weight percentage was increased from 25 to 50 wt%. From the PLSF-VE composite with very low filler content, the percentage of elongation at break was very low, which indicated the brittle nature of the composites.

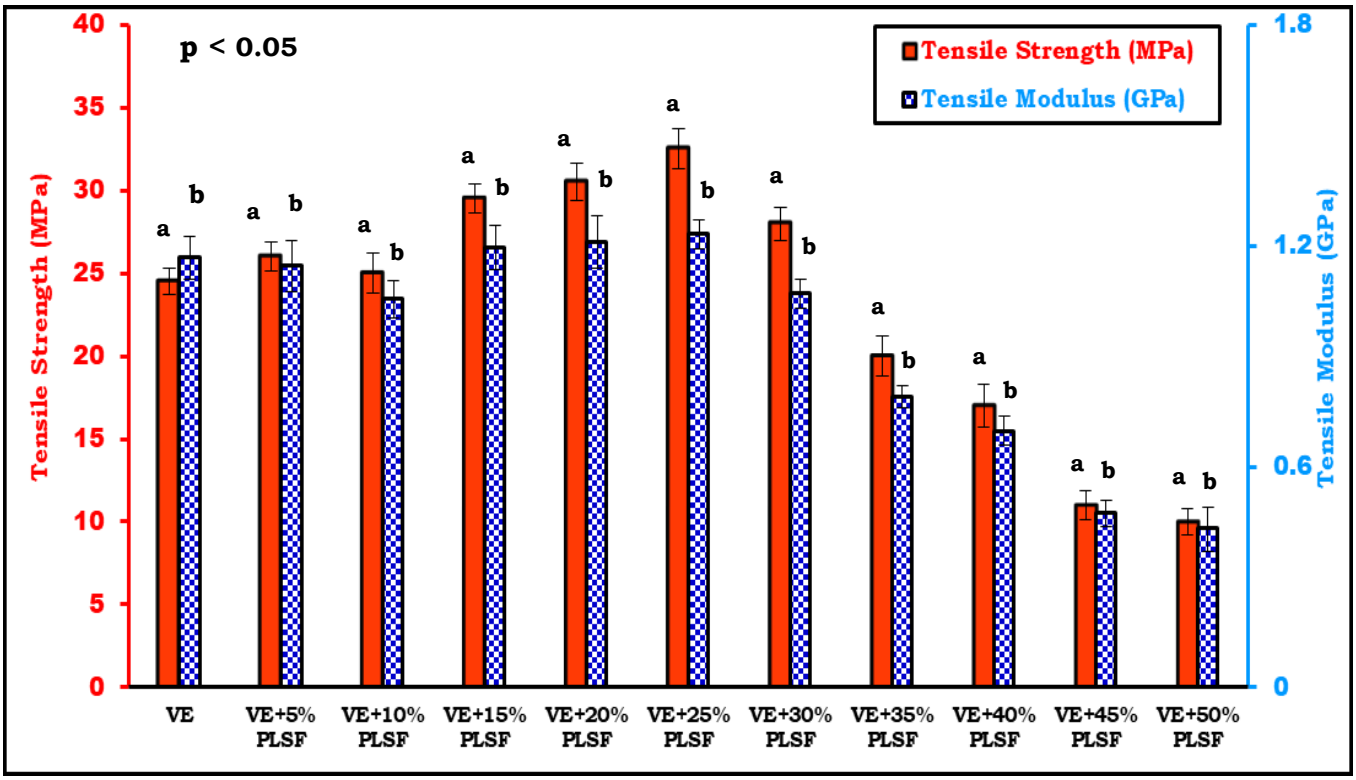

Fig. 3(a). Effects of filler loadings on tensile strengths and moduli of the various samples. Different superscript letters indicate significant differences ($p<0.05$).

The PLSF-VE composites exhibited an increase in the percentage of elongation at break from 2.1 to 2.64% by varying filler weight from 5 to 50%. It was evident that the addition of PLSF to the vinyl ester matrix reduced its brittle nature; slightly changed the brittle property towards uncommon ductile nature of the PLSF-VE composite samples. Furthermore, the PLSF-VE composites recorded a greater tensile strength, when compared with some similar natural fiber or filler reinforced polymer (FRP) composite samples (Table 1). For instance, PLSF-VE composites were 1.17, 1.25, 2.09 and 2.59 times higher than that of composites of pistachio nutshell filler/poly (lactic acid), wood filler/epoxy, almond nutshell filler/poly (lactic acid) and walnut nutshell filler/poly (lactic acid) (Sutivisedsak et al., 2012; Kumar et al., 2018; Sutivisedsak et al., 2012; Zheng et al., 2019), respectively.

Table 1. Comparison of mechanical properties of the *Polyalthia longifolia* seed filler/vinyl ester (PLSF-VE) composite with other fillers and fibers-based composites.

Composite materials	Manufacturing process	Tensile strength (MPa)	Flexural strength (MPa)	Impact strength (kJ/m^2)	Hardness	Reference
Polyalthia longifolia seed filler/vinyl ester	Compression molding	9 – 32.5	44 – 125	10 – 31.09	23 – 36.5	Present work
Date seed filler/vinyl ester	Compression molding	10.5 – 40.3	46 – 149	9.43 – 17.03	20.33 – 51	(Nagaprasad et al., 2019)
Palm kernel shell/unsaturated polyester resin	Hand lay-up	2 – 20	5 – 38	3.5 – 5	10 – 15	(Adeosun et al., 2016)
Sugarcane bagasse/unsaturated polyester resin	Hand lay-up	2 –24	18 – 50	3.5 – 7	8 – 14	(Adeosun et al., 2016)
Pineapple chaffs/unsaturated polyester resin	Hand lay-up	2 – 23	9 – 38	3.5 – 5.2	9 – 13	(Adeosun et al., 2016)
Pecan nutshell/poly lactic acid	Injection molding	61	109	--	--	(Sánchez-Acosta et al., 2019)
Pistachio nutshell filler/poly (lactic acid)	Injection molding	8 – 29.2	--	--	--	(Sutivisedsak et al., 2012)
Almond nutshell filler/poly (lactic acid)	Injection molding	10 – 16.2	--	--	--	(Sutivisedsak et al., 2012)
Sewage sludge ash/polyester	Hand lay-up	40 – 50.2	73 – 107.2	--	--	(Erkliğ et al., 2016)
Fly ash/polyester	Hand lay-up	41 – 51.9	82 – 109.9	--	--	(Erkliğ et al., 2016)

wood filler/epoxy	Hand lay-up	6 – 27.8	--	--	--	(Kumar et al., 2018)
Thyme herbs/polyethylene	Injection molding	19 – 24	23 – 36	2 – 3.3	53 – 60	(Montanes et al., 2018)
Tamarind seed filler/vinyl ester	Compression molding	9 – 34.1	47 – 121	7 – 14	23 – 42.33	(Stalin et al., 2019)
Roselle/sugar palm fiber/vinyl ester	Hand lay-up	15 – 24.65	58 – 110	--	--	(Razali, Sapuan, & Razali, 2018)
Betel nut husk fiber/vinyl ester	Compression molding	39 – 100	60 – 80	2 – 5.7	--	(Akil et al., 2009)
Sisal fiber/epoxy	Hand lay-up	5 – 15.64	22 – 60.89	5 – 13.24	--	(Owen, Ogunleye, & Achukwu, 2015)
Nappier grass fiber/epoxy	Hand lay-up	21 – 39.53	45 – 76.21	--	--	(Kommula, Reddy, Shukla, Marwala, & Rajulu, 2014)
Glass fiber/banana chopped filler/polyester	Hand lay-up	41 – 45	80 – 90	--	--	(Gupta, Gupta, Dhanola, & Raturi, 2016)
Glass fiber/rice husk/polyester	Hand lay-up	41 – 43	80 – 83	--	--	(Gupta et al., 2016)
Carbon fiber/cement by-pass dust/vinyl ester	Gravity casting method	10 – 18.5	28 – 34.5	--	--	(Gangil, Patnaik, & Kumar, 2013)

3.2.2 Flexural strength

The flexural strengths and moduli of the various samples are depicted in Fig. 3(b). Addition of PLSF to the vinyl ester matrix used (neat resin) increased or improved the flexural strengths of the various PLSF-VE composite samples up to a filler loading of 35 wt%. The increasing trend was more prominent between the filler contents of 15 and 25 wt%. Similarly, the flexural modulus of the PLSF-VE composite was enhanced when vinyl ester matrix was reinforced with PLSF material. Flexural strength of 78 MPa and modulus of 3.64 GPa were recorded by the vinyl ester. By adding 5 wt% of PLSF to the matrix, the flexural strength of 100.4 MPa was increased by 28.72%. Meanwhile, when the filler loading percentage was increased from 5 to 10 and 15 wt%, the flexural strengths of the PLSF-VE composites were respectively decreased from 100.4 to 84 and 92 MPa. But, beyond 15 wt%, the flexural strength was gradually increased up to 35 wt% of PLSF reinforced composites. With 20 wt% filler loading, a sudden increase was observed, due to the PLSF content which reduced a quite amount of brittle property of the vinyl ester matrix. Significantly, the 25 wt% PLSF composite achieved the maximum flexural strength behavior of 125 MPa. Hence, it was evident that 25 wt% PLSF-VE composite recorded an optimum value, which was 60.26% higher than the neat vinyl ester resin. This can be attributed to the proper reinforcement-matrix interfacial adhesion. The flexural properties (strength and modulus) of the composite started to decrease immediately after the threshold value of 25 wt% and reduced much more with 35 wt% filler loading and other higher contents. This can be traced to an occurrence of weak interfacial bonding between higher contents of PLSF and vinyl ester resin. The flexural strength of PLSF-VE composite was 14.68, 56.25, 105.29, 262.32 and 247.22% higher than that of pecan nutshell/polylactic acid, betel nut husk fiber/vinyl ester, sisal fiber/epoxy, carbon fiber/cement by-pass dust/vinyl ester and thyme herbs/polyethylene composites (Sánchez-Acosta et al.,

2019; Akil et al., 2009; Owen, Ogunleye, & Achukwu, 2015; Gangil, Patnaik, & Kumar, 2013; Montanes et al., 2018), respectively.

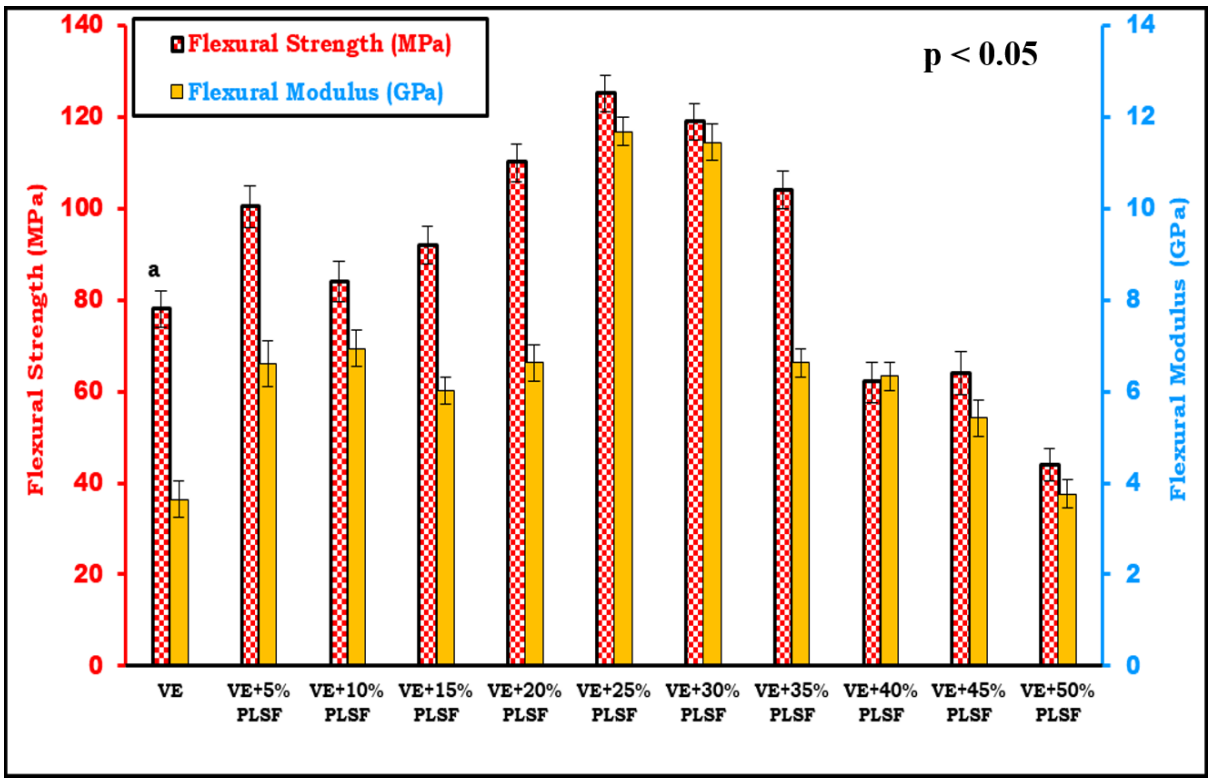

Fig. 3(b). Effects of filler loadings on flexural strengths and moduli of the various samples. Different superscript letters indicate significant differences ($p<0.05$).

3.2.3 Impact strength

The capability of a material to resist or withstand a suddenly applied load is referred to as impact strength. While, the ability of a workpiece to resist plastic deformation under an indenter is known as hardness. Fig. 3(c) depicts the impact strength and hardness properties of the various samples. The impact strength of pure vinyl ester resin was 11.83 kJ/m^2. But, it was increased to 13.50, 23.91 and 26.24 kJ/m^2 after respectively reinforced with filler contents of 5, 10 and 15 wt%. It was evident from the experimental results obtained that an improvement in impact strength was recorded up to 45 wt% of PLSF content. However, there was a significant decrease with 50 wt% PLSF-VE composite. It was therefore evident that the

maximum or optimum impact strength was recorded with the 25 wt% PLSF-VE composite. The improved interfacial property of PLSF-VE composite supported its increased impact strength by 1.83, 2.22, 2.35, 5.45 and 9.42 times higher than that of date seed filler/vinyl ester, tamarind seed filler/vinyl ester, sisal fiber/epoxy, betel nut husk fiber/vinyl ester and thyme herbs/polyethylene composites (Nagaprasad et al., 2019; Stalin et al., 2019; Owen, Ogunleye, & Achukwu, 2015; Akil et al., 2009; Montanes et al., 2018), respectively.

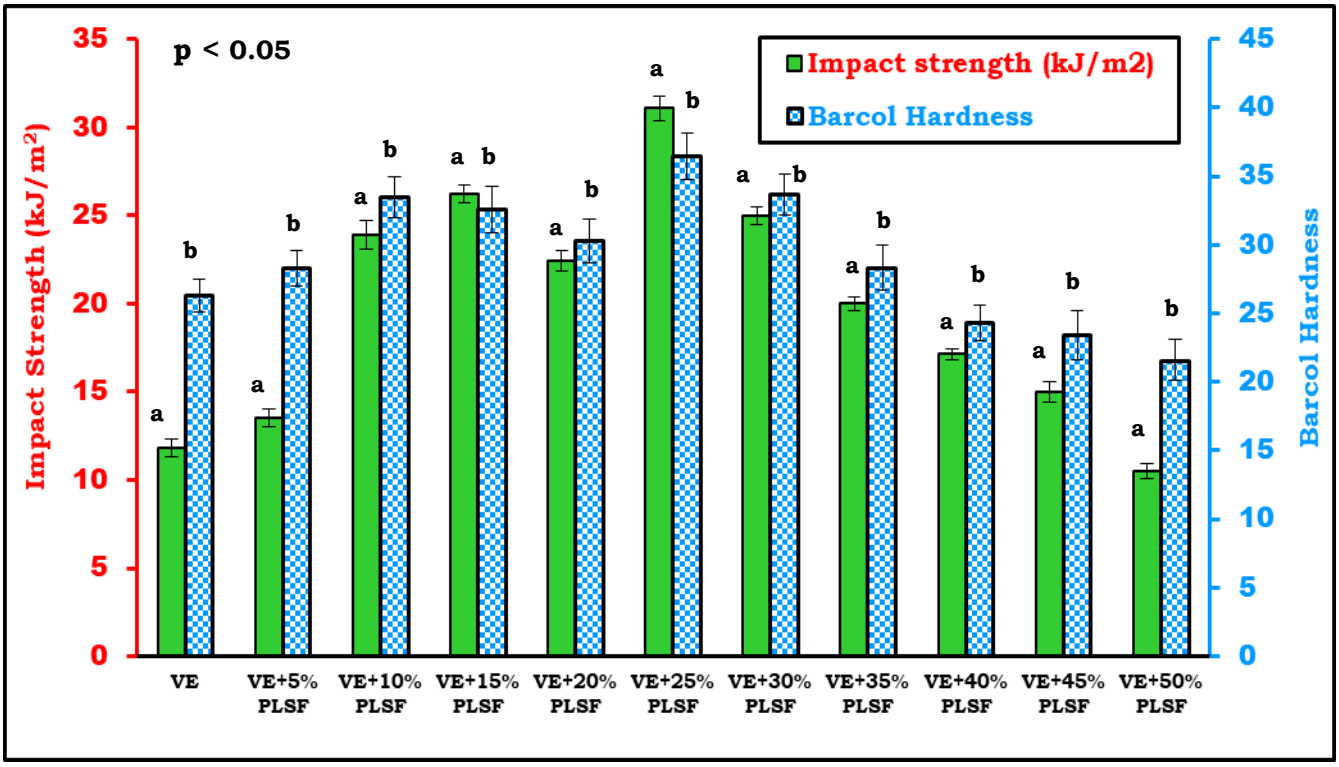

Fig. 3(c). Effects of filler loadings on impact strengths and hardness of the various samples. Different superscript letters indicate significant differences ($p<0.05$).

3.2.4 Hardness property

An increase in the PLS filler loadings resulted to an increase in the hardness values of the composites. The neat vinyl ester resin recorded a hardness value of 26.33. It was observed from the results obtained (Fig. 3(c)) that the hardness values increased from 26.33 to an optimum value of 36.5 with 25 wt% PLSF reinforced composite sample, and up to 35 wt% of

filler content. Afterwards, the hardness value decreased up to 50 wt% of filler loadings. The observed increase in the hardness value, as a function of filler loading, especially with 25 wt% of filler content can be ascribed to the even distribution of the filler particles and a good filler-matrix interfacial bonding. These reduced the penetration of the indenter on the surfaces of the PLSF reinforced composite test specimens.

3.3 Microstructural examination

Fig. 4 depicts the SEM micrographic surfaces of the PLSF-VE fractured specimens, after tensile tests. The morphology in Fig. 4(a) shows that there were occurrences of filler pull-out and cavity formation on the 40 wt% PLSF-VE composite specimen fractured surfaces. Consequently, micro cracks were simply spread on the vinyl ester matrix. It later exhibited poor tensile strength. The resultant poor filler-matrix interfacial strength caused an ineffective stress transfer. In Fig. 4(b), a few filler accumulations were observed and filler was completely wetted with the matrix. It supported the excellent adhesion between filler and matrix. There was no filler pull-out that predominantly occurred. Consequently, it was observed that 25 wt% PLSF-VE composite produced a maximum tensile strength. This excellent performance was attributed to the effective filler-matrix stress transfer within the composite structure.

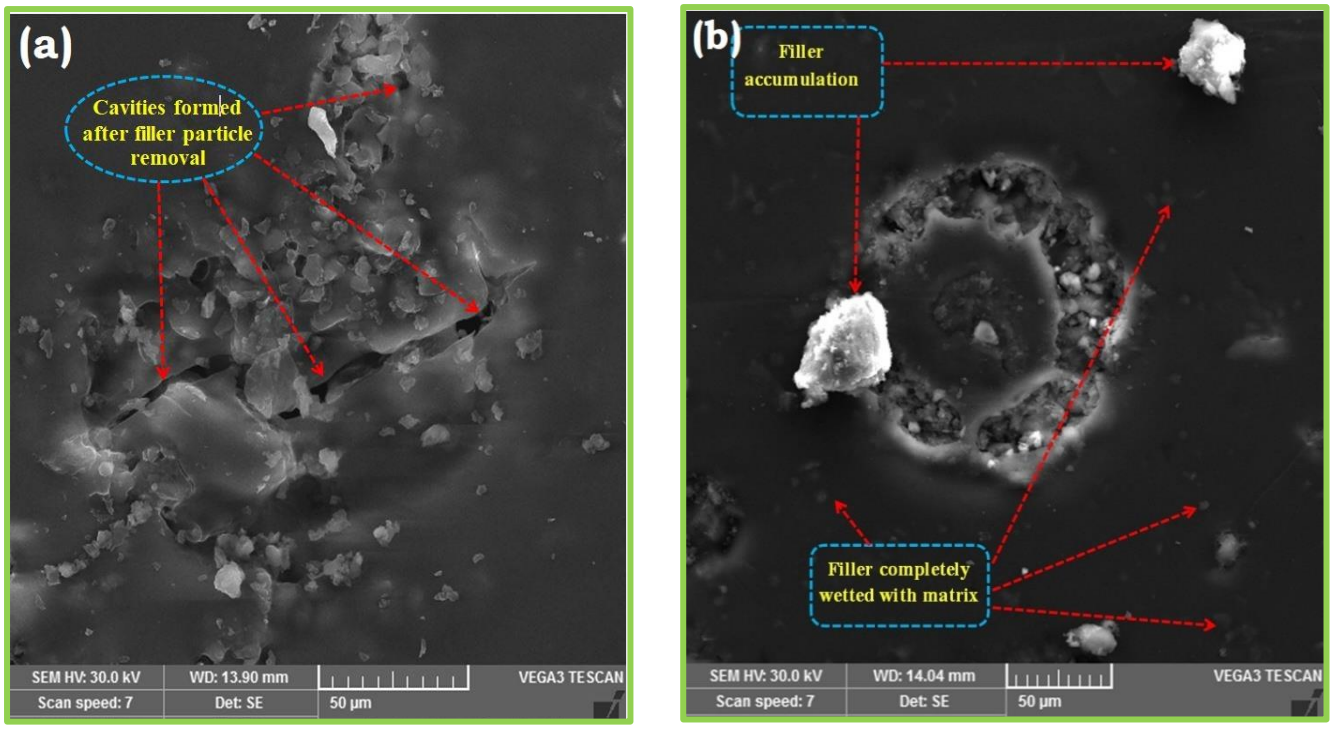

Fig. 4. SEM images of fractured tensile specimens of PLSF-VE composites with filler contents of (a) 40 and (b) 25 wt%.

Moreover, the SEM micrographic fractured PLSF-VE specimens, after subjected to the flexural strength test, are shown in Fig. 5. From Fig. 5(a), an increased amount of filler accumulation and filler pull-out were observed on the 40 wt% PLSF-VE fractured composite surfaces, because of the poor adhesion. Filler pull-out on the matrix was due to the mechanical interlocking, while filler-matrix interfacial adhesion strength depended on the filler-matrix inter-diffusion level (Kommula et al., 2014; Owen et al., 2015). From Fig. 5(b), better bonding between filler and the matrix was observed, with the presence of a very few voids with 25 wt% of filler loadings. This resulted in a maximum flexural strength of the 25 wt% PLSF-VE composite sample.

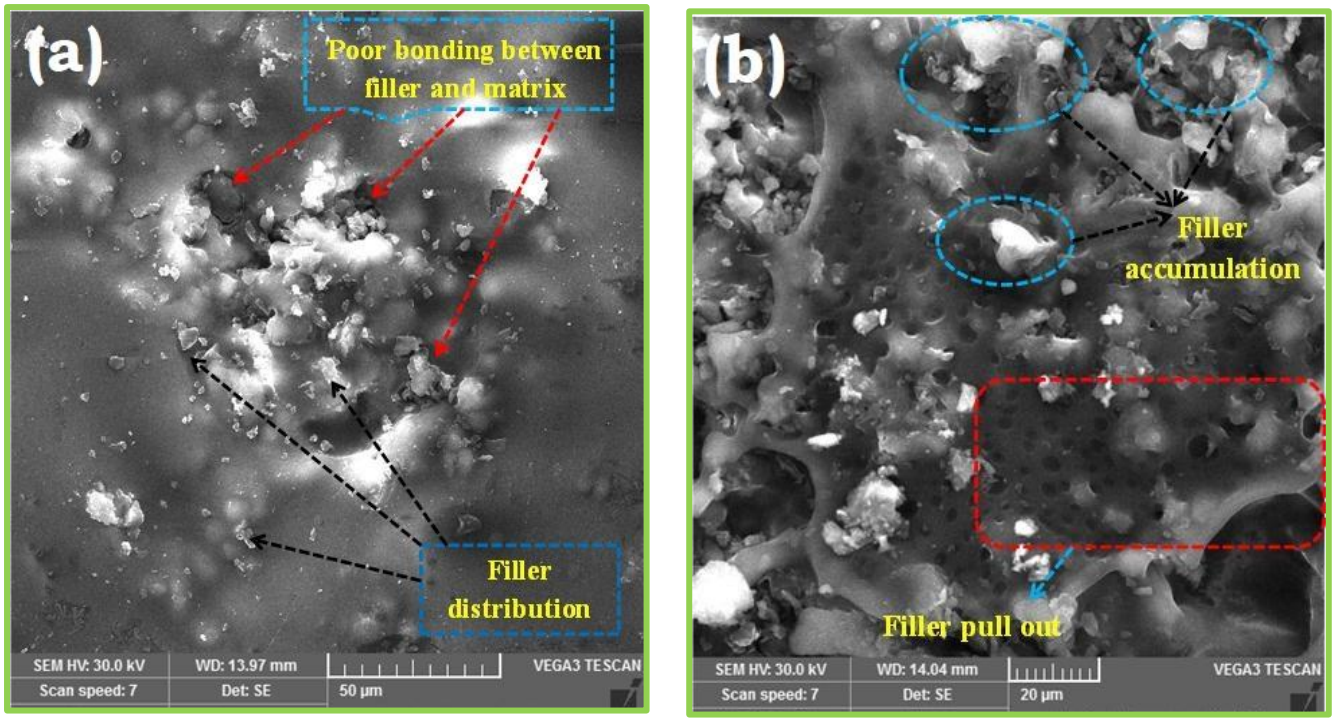

Fig. 5. SEM micrographs of fractured flexural specimens of PLSF-VE composites with filler contents of (a) 40 and (b) 25 wt%.

The cross-sectional surfaces of the PLSF-VE impact fractured composites were analyzed. The SEM micrographs of the composite samples are shown in Fig. 6. Fig. 6(a) shows the composite with 25 wt% of PLS filler loadings, indicating excellent interaction between the filler and vinyl ester resin. Therefore, the formation of voids within the composite sample was reduced. Also, this reflected in the excellent impact strength of the 25 wt% PLSF-VE composite. Fig. 6(b) depicts the 50 wt% PLS filler loaded composites. An increase in the filler loading resulted to a decrease in the quantity of matrix within the composite system. Therefore, de-bonding, voids, weak interfacial bonding and filler pull-out occurred. Reinforcing particle or filler usually pulls out as a replacement for fracture whenever there is either ineffective particle/fiber-matrix interaction or weak interface, or both. Hence, it decreased the structural capability, including mechanical behaviors of the composite (Sánchez-Acosta et al., 2019). Composites with a higher percentage of filler loading reduced the plastic region of the

composites and consequently, resulted to a brittle failure, as shown in Fig. 6(b) and a decrease in the impact strength (Richard et al., 2016).

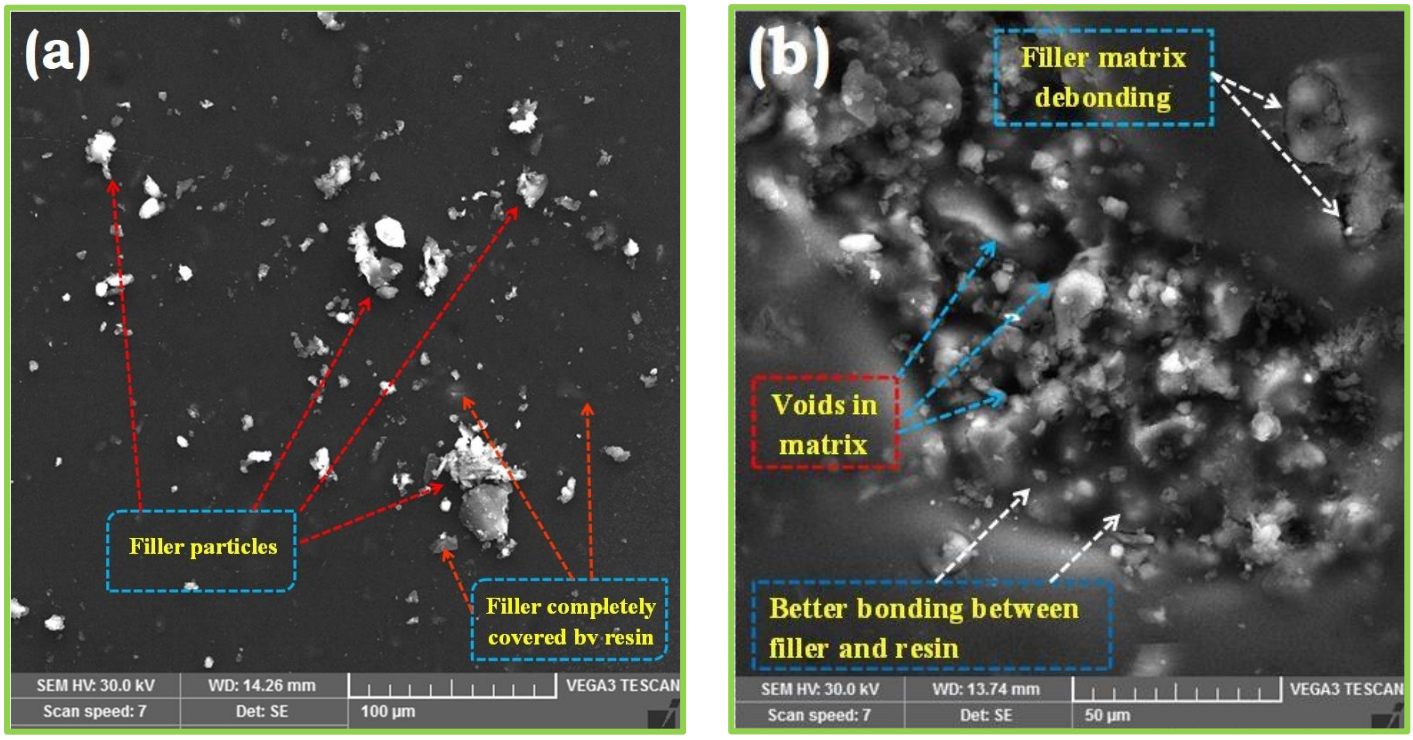

Fig. 6. SEM micrographs of fractured impact specimens of PLSF-VE composites with filler contents of (a) 25 and (b) 50 wt%.

3.4 Thermal analysis

3.4.1 Heat deflection temperature

A measured temperature that causes a material to deflect by 0.25 mm when subjected to a load of 455 kPa is technically referred to as a heat deflection temperature (HDT); simply called a softening point of a material. It is an essential factor usually considered by the industrial designers of polymer-based engineering components. All the samples recorded different HDT values, as depicted in Fig. 7. The HDT value of neat vinyl ester resin (with 0 wt% filler content) was 53 ^{o}C. The HDT value of PLSF-VE samples steeply increased when there was an increase in the filler weights. Precisely, with 10 wt% of PLSF, the HDT was 17% much greater than that of the pure resin. The HDT of 25 wt% PLSF-VE composite significantly

increased to a maximum value of 66 ºC. This value was 24.53% greater when compared with the value recorded from the neat vinyl ester resin. Importantly, a continuous decrease in the HDT was observed when the filler content was increased above 25 wt%.

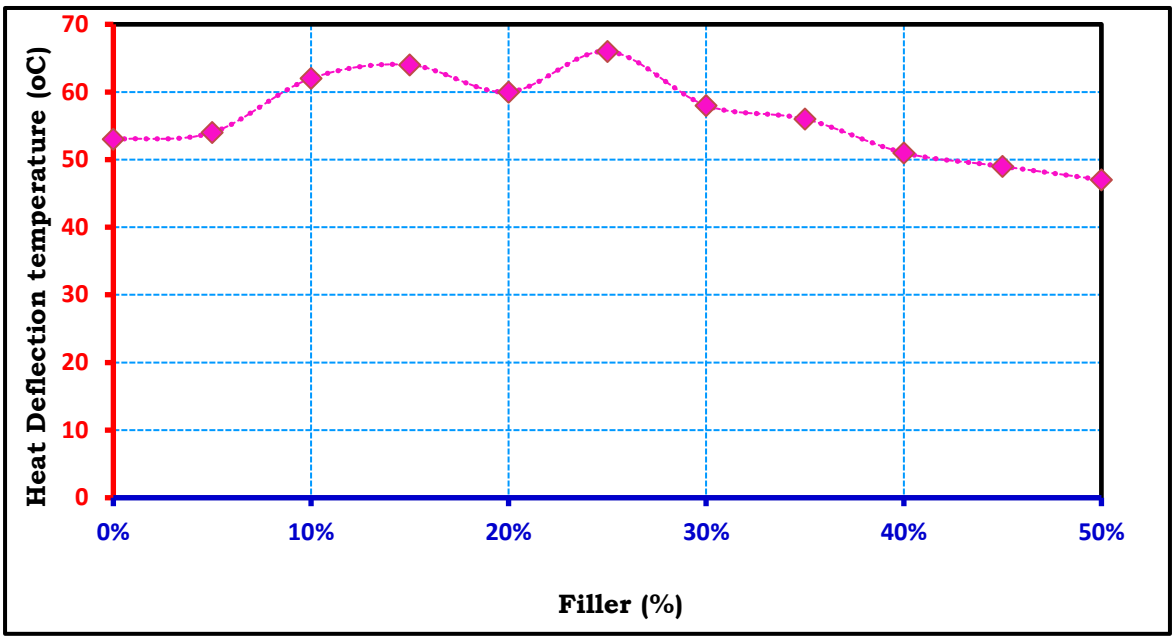

Fig. 7. Heat deflection temperature *versus* filler loadings of the various samples.

3.4.2 Thermo-gravimetric and differential thermal analyses

Thermal stability and degradation behaviors of both PLS filler and PLSF-VE composites were determined using TGA. Figs. 8(a)-(d) show the thermal degradation profiles obtained from the TGA as well as DTA curves of the PLS filler, neat vinyl ester resin, PLSF-VE samples with filler contents of 25 and 50%, respectively. There was an increase in temperature from 25 °C to 1000 °C for the various components of the specimens to burn and the percentage of the mass loss in each specimen was measured. The test results depicted three phases of thermal degradation. The stage 1 of the dehydration process was observed below 150 °C, stage 2 was between 150 and 400 °C and followed by the last stage below 400 °C. The inception stage of PLS filler thermal degradation was recorded above 95 °C and major weight loss was occurred

between 290 and 310 °C. The pure vinyl ester resin recorded thermal stability up to 385 °C. The resin exhibited a major weight loss between 300 and 385 °C. The 25 and 50 wt% PLSF-VE composite samples recorded different major weight losses at 430 °C and 410 °C, respectively. Summarily, the thermal stability of PLSF-VE composite was 11.69% higher than that of the neat vinyl ester resin.

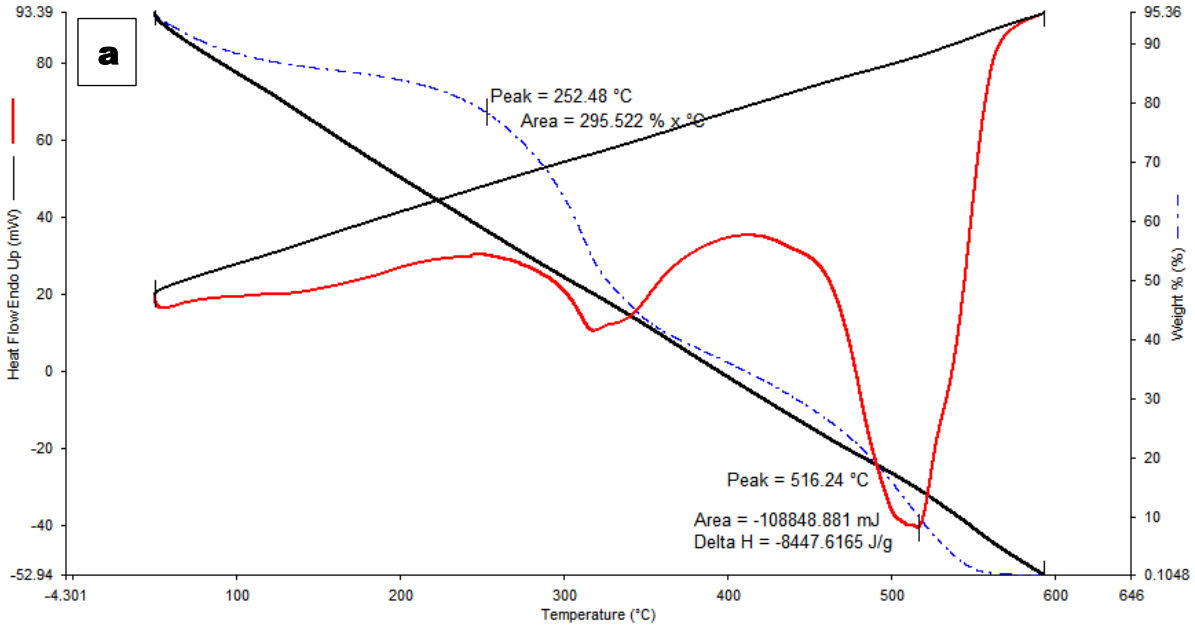

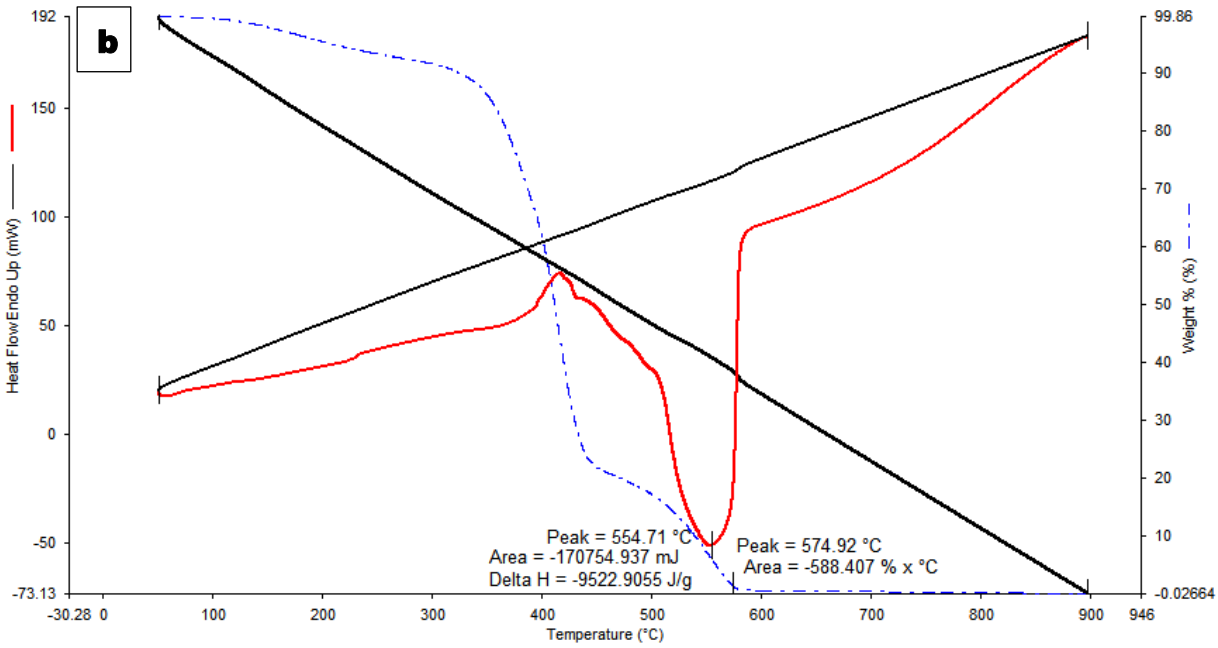

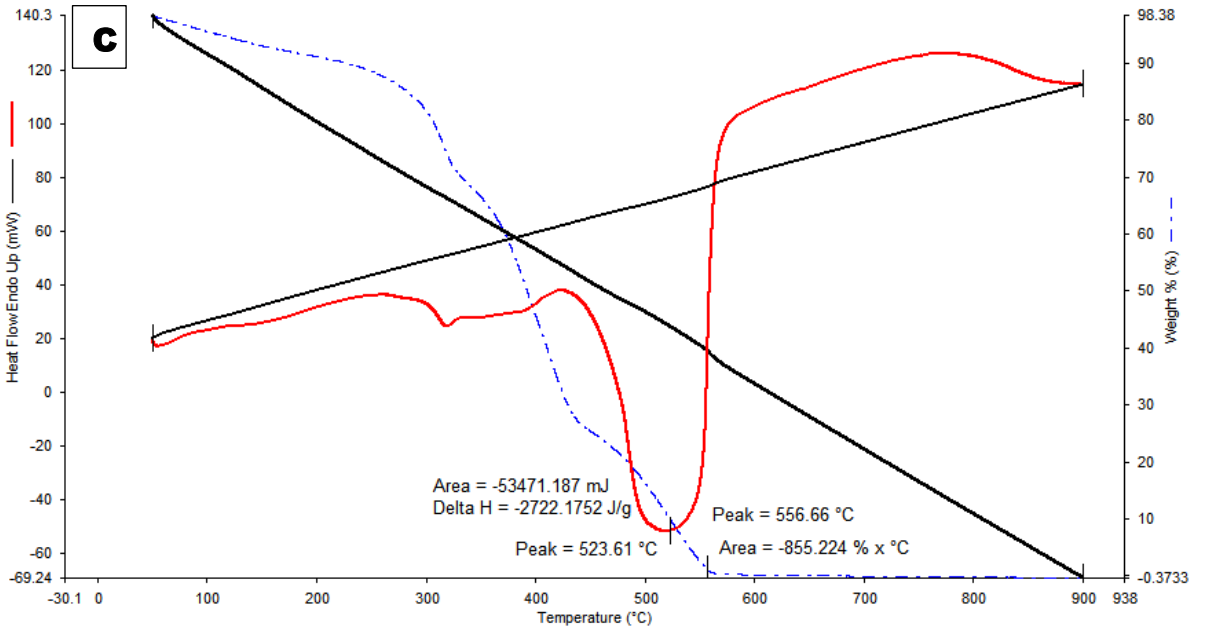

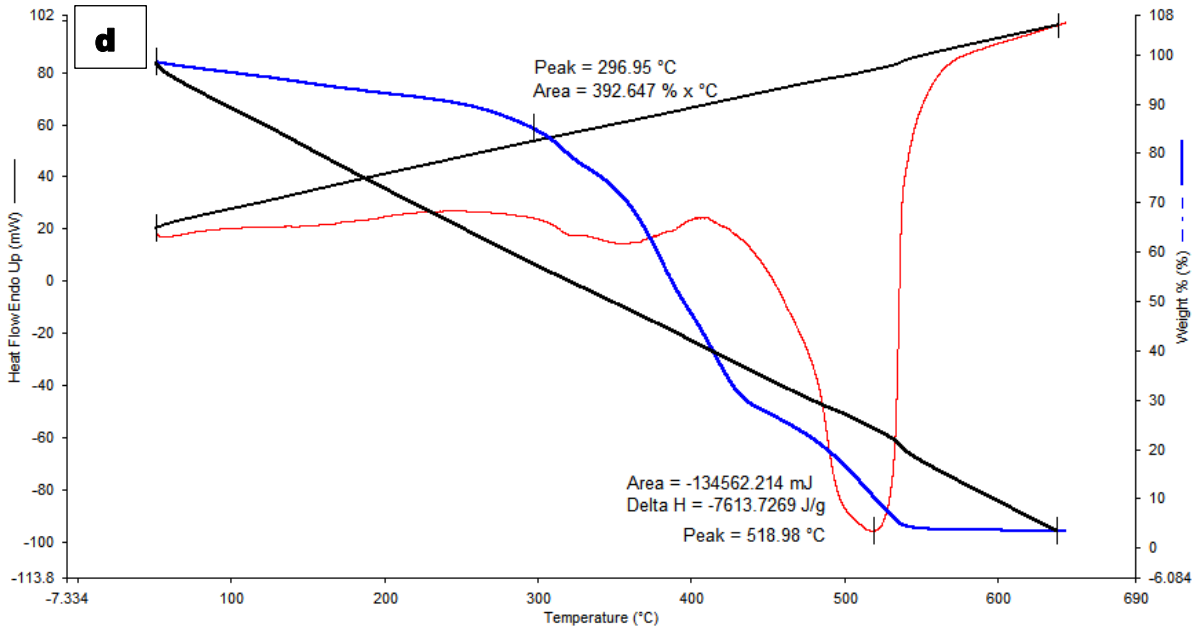

Fig. 8. TGA and DTA curves of (a) PLS filler, (b) neat vinyl ester resin, (c) 25 and (d) 50 wt% filler loadings.

3.5 Water absorption behavior

The water absorption behaviors of the various samples under normal, salt, hot and cold water conditions are presented in Fig. 9. An increase in the water absorption was observed when there was an increase in the PLSF loadings, as shown in the moisture absorption curve. This was attributed to the hydrophilicity property of the PLSF material. The hydrophobic nature of the resin supported the lower quantity of water absorption exhibited by the composite samples with lower filler contents (5 - 25 wt%); they were richer in resin when compared with higher filler reinforced composites (above 25 wt%). After 25 wt% PLSF loading, the water absorption percentage was increased, as a result of the existence of more microvoids and less vinyl ester resin (much hydrophilic filler) in the composite samples. It was evident from Fig. 9 that the absorption percentage was very small, till an optimal content of 25 wt%. The best performance can be traced to the good filler-matrix interaction, which caused a reduction in the movement or speed of the diffusing particles. Expectedly, there was an increase in the diffusivity process of the composite samples in the hot water. Therefore, it recorded the maximum percentage of water absorption, when compared with the other three environments. A similar trend of result has been reported for the same vinyl ester matrix when reinforced with tamarind seed filler to produce various similar biocomposites (Stalin et al., 2019). Nevertheless, in the sea or saltwater, a slow penetration occurred. This was traced to the occurrence of large salt (notable sodium chloride) molecules. Therefore, it absorbed less water, similar to that of normal water. Among the four environmental conditions, PLSF composite immersed in normal water recorded the least value of water absorption.

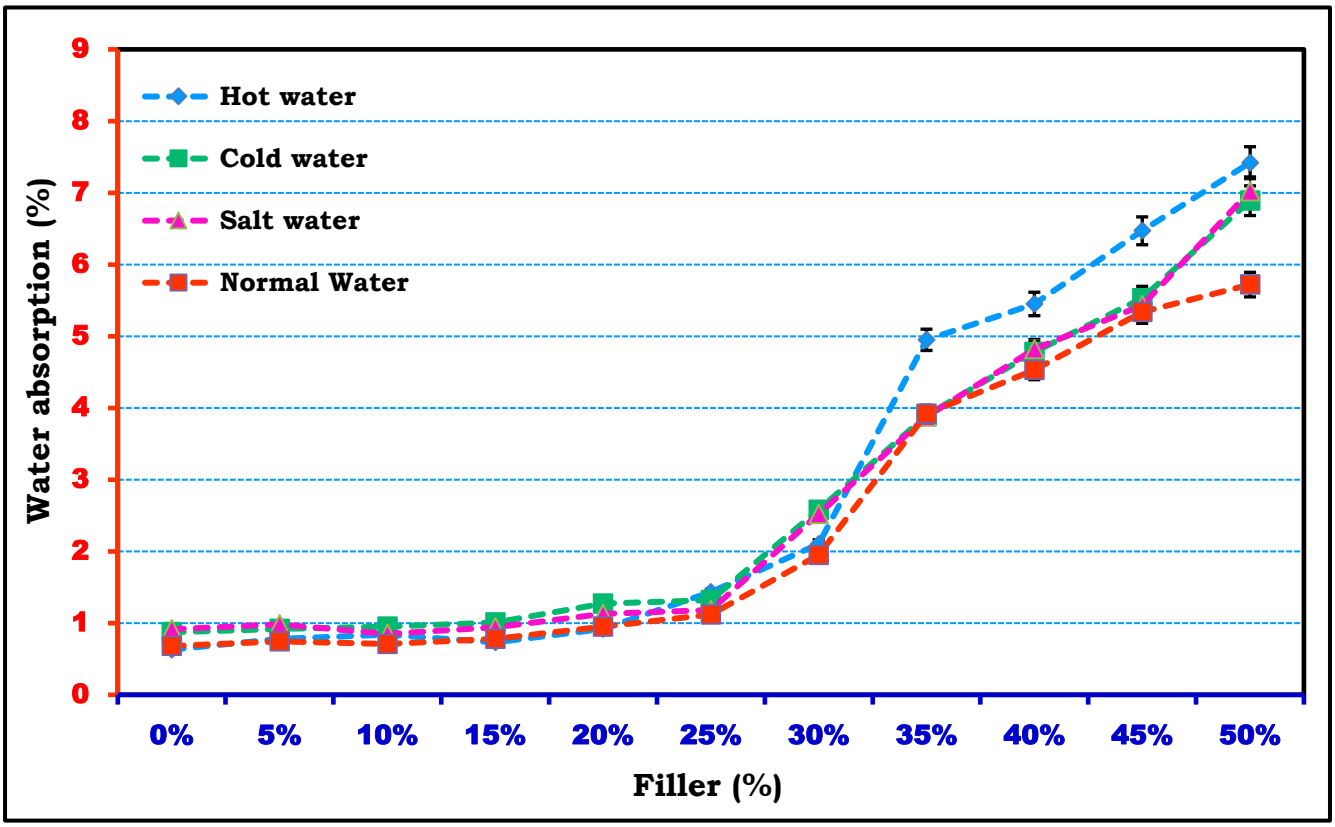

Fig. 9. Water absorption behaviors of the various samples under different aqueous environments.

4. Conclusions

The characterization of *Polyalthia longifolia* seed bio-filler as well as mechanical, thermal and water absorption behaviors of the PLSF/VE composite samples with varied filler loadings of 5 – 50 wt% have been experimentally and extensively investigated. Therefore, the following conclusions were drawn from the results obtained.

- The tensile strength of the PLSF-VE composite samples increased with the filler loadings up to 30 wt%, afterwards the tensile strength decreased, due to the poor interfacial adhesion between the filler and matrix. This was evident from the SEM analysis. The maximum tensile strength and modulus of the PLSF-VE composite were 32.50 MPa and 1.23 GPa, respectively.

- The flexural and impact strengths of the PLSF-VE samples were also extensively influenced by the addition of filler, up to 35 wt%. The flexural and impact strengths of the PLSF-VE composites were increased by 1.60 and 2.63 times than that of neat vinyl ester resin, respectively. The barcol hardness of the pure vinyl ester resin was 26.33, but it increased by 38.61% after adding PLS filler content of 25 wt%.
- The thermal stability of the biocomposite sample was slightly enhanced by adding PLS filler to the vinyl ester resin.
- Moreover, the water absorption test results indicated that the percentage of water absorption followed a similar trend and was less in all the four environments considered or water treatments, up to 25 wt% filler loadings. This was attributed to the existence of a better filler-matrix interfacial bonding when compared with other filler loadings, especially those with higher values.
- Summarily, it was evident that the optimum values from the investigated mechanical, thermal and water absorption behaviors of the PLSF-VE composite samples occurred with filler loading of 25 wt%.

Acknowledgements

We hereby acknowledge and sincerely appreciate unalloyed supports from the managements of the following institutions: ULTRA College of Engineering and Technology, Anna University, Regional Campus Madurai as well as the Sethu Institute of Technology, Tamil Nadu, India.

References

Abhishek, S., Sanjay, M. R., George, R., Siengchin, S., Parameswaranpillai, J., & Pruncu, C. I. (2018). Development of new hybrid *Phoenix pusilla*/carbon/fish bone filler reinforced polymer composites. *Journal of the Chinese Advanced Materials Society*, *6*(4), 553–560.

Akil, H. M., Cheng, L. W., Ishak, Z. A. M., Bakar, A. A., & Rahman, M. A. A. (2009). Water absorption study on pultruded jute fibre reinforced unsaturated polyester composites. *Composites Science and Technology*, *69*(11–12), 1942–1948.

Adeosun, S. O., Gbenebor, O, P., Akpan, E. I., & Udeme, F. A. (2016). Influence of organic fillers on physicochemical and mechanical properties of unsaturated polyester composites. *Arabian Journal for Science and Engineering*, *41*(10), 4153-4159.

Balaji, A. N., Karthikeyan, M. K. V, & Vignesh, V. (2016). Characterization of new natural cellulosic fiber from kusha grass. *International Journal of Polymer Analysis and Characterization*, *21*(7), 599–605.

Battegazzore, D., Noori, A., & Frache, A. (2019). Natural wastes as particle filler for poly (lactic acid)-based composites. *Journal of Composite Materials*, *53*(6), 783–797.

Bensalah, H., Gueraoui, K., Essabir, H., Rodrigue, D., Bouhfid, R., & Qaiss, A. el kacem. (2017). Mechanical, thermal, and rheological properties of polypropylene hybrid composites based clay and graphite. *Journal of Composite Materials*, *51*(25), 3563–3576.

Conrad, C. M., 1944. Determination of wax in cotton fiber, a new alcohol extraction method. *Industrial and Engineering Chemistry Analytical Edition*, *16*, 745–748.

Dixit, P., Mishra, T., Pal, M., Rana, T. S., & Upreti, D. K. (2014). *Polyalthia longifolia* and its pharmacological activities. *International Journal of Scientific and Innovative Research*, *2*(1), 17–25.

Erdogan, S., & Huner, U. (2018). Physical and mechanical properties of PP composites based on different types of lignocellulosic fillers. *Journal of Wuhan University of Technology-*

Materials Science Edition, *33*(6), 1298–1307.

Erkliğ, A., Alsaadi, M., & Bulut, M. (2016). A comparative study on industrial waste fillers affecting mechanical properties of polymer-matrix composites. *Materials Research Express*, *3*(10), 105302.

Gangil, B., Patnaik, A., & Kumar, A. (2013). Mechanical and wear behavior of vinyl ester-carbon/cement by-pass dust particulate filled homogeneous and their functionally graded composites. *Science and Engineering of Composite Materials*, *20*(2), 105–116.

Gopinath, R., Ganesan, K., Saravanakumar, S. S., & Poopathi, R. (2016). Characterization of new cellulosic fiber from the stem of *Sida rhombifolia*. *International Journal of Polymer Analysis and Characterization*, *21*(2), 123–129.

Gupta, G., Gupta, A., Dhanola, A., & Raturi, A. (2016). Mechanical behavior of glass fiber polyester hybrid composite filled with natural fillers. *IOP Conference Series: Materials Science and Engineering*, *149*(1), 012091.

Karthikeyan, M. K. V., Balaji, A. N., & Vignesh, V. (2016). Effect of rope mat and random orientation on mechanical and thermal properties of banana ribbon-reinforced polyester composites and its application. *International Journal of Polymer Analysis and Characterization*, *21*, 296-304.

Kommula, V. P., Reddy, K. O., Shukla, M., Marwala, T., & Rajulu, A. V. (2014). Mechanical properties, water absorption, and chemical resistance of Napier grass fiber strand–reinforced epoxy resin composites. *International Journal of Polymer Analysis and Characterization*, *19*(8), 693–708.

Kumar, R., Kumar, K., & Bhowmik, S. (2018). Mechanical characterization and quantification of tensile, fracture and viscoelastic characteristics of wood filler reinforced epoxy composite. *Wood Science and Technology*, *52*(3), 677–699.

Montanes, N., Garcia-Sanoguera, D., Segui, V. J., Fenollar, O., & Boronat, T. (2018).

Processing and characterization of environmentally friendly composites from biobased polyethylene and natural fillers from thyme herbs. *Journal of Polymers and the Environment*, *26*(3), 1218–1230.

Mayandi, K., Rajini, N., Pitchipoo, P., Sreenivasan, V.S., Jappes, J. T. W., & Alavudeen, A. (2015). A comparative study on characterisation of *Cissus quadrangularis* and *Phoenix reclinata* natural fibers. *Journal of Reinforced Plastics and Composites*, *34*(4), 269–280.

Najafi, S. K., Kiaefar, A., Hamidina, E., & Tajvidi, M. (2007). Water absorption behavior of composites from sawdust and recycled plastics. *Journal of Reinforced Plastics and Composites*, *26*(3), 341–348.

Nagaprasad, N., Stalin, B., Vignesh, V., Ravichandran, M., Rajini, N., & Ismail, O. (2020). Effect of cellulosic filler loading on mechanical and thermal properties of date palm seed / vinyl ester composites. *International Journal of Biological Macromolecules*, *147*, 53-66.

Nagarajan, K. J., & Balaji, A. N. (2016). Extraction and characterization of alkali-treated red coconut empty fruit bunch fiber. *International Journal of Polymer Analysis and Characterization*, *21*(5), 387–395.

Nagarajan, K. J., Balaji, A. N., Rajan, S. T. K., & Ramanujam, N. R. (2020). Preparation of bio-eco based cellulose nanomaterials from used disposal paper cups through citric acid hydrolysis. *Carbohydrate Polymers*, *235*, 115997.

Owen, M. M., Ogunleye, C. O., & Achukwu, E. O. (2015). Mechanical properties of sisal fibre-reinforced epoxy composites-effect of alkali concentrations. *Advanced Polymer Science and Technolgy*, *5*, 26–31.

Pillai, G. P., Manimaran, P., & Vignesh, V. (2020). Physico-chemical and mechanical properties of alkali-treated red banana peduncle fiber. *Journal of Natural Fiber*, doi:10.1080/15440478.2020.1723777.

Pongdong, W., Kummerlöwe, C., Vennemann, N., Thitithammawong, A., & Nakason, C. (2018). A comparative study of rice husk ash and siliceous earth as reinforcing fillers in epoxidized natural rubber composites. *Polymer Composites*, *39*(2), 414–426.

Rao, R. A. K., & Rehman, F. (2012). Use of *Polyalthia longifolia* seeds (seeds of Indian Mast tree) as adsorbent for the removal of Cd(II) from aqueous solution. *Journal of Dispersion Science and Technology*, *33*(4), 472–481.

Razali, N., Sapuan, S. M., & Razali, N. (2018). Mechanical properties and morphological analysis of Roselle/sugar palm fiber reinforced vinyl ester hybrid composites. *In Natural fibre reinforced vinyl ester and vinyl polymer composites* (pp. 169–180). Elsevier.

Richard, S., Rajadurai, J. S., & Manikandan, V. (2016). Influence of particle size and particle loading on mechanical and dielectric properties of biochar particulate-reinforced polymer nanocomposites. *International Journal of Polymer Analysis and Characterization*, *21*(6), 462–477.

Richard, S., Selwin Rajadurai, J., Manikandan, V., Thanu, M. C., Arumugaprabu, V., & Johnson, R. D. J. (2019). Study of tribological properties of nano-sized red mud particle-reinforced polyester composites. *Transactions of the Indian Institute of Metals*, *72*(9), 2417–2431.

Sánchez-Acosta, D., Rodriguez-Uribe, A., Álvarez-Chávez, C. R., Mohanty, A. K., Misra, M., López-Cervantes, J., & Madera-Santana, T. J. (2019). Physicochemical characterization and evaluation of pecan nutshell as biofiller in a matrix of poly (lactic acid). *Journal of Polymers and the Environment*, *27*(3), 521–532.

Sathishkumar, T. P., Navaneethakrishnan, P., & Shankar, S. (2012). Tensile and flexural properties of snake grass natural fiber reinforced isophthallic polyester composites. *Composites Science and Technology*, *72*(10), 1183–1190.

Sreenivasan, V. S., Somasundaram, S., Ravindran, D., Manikandan, V., & Narayanasamy, R.

(2011). Microstructural, physico-chemical and mechanical characterisation of *Sansevieria cylindrica* fibres–An exploratory investigation. *Materials & Design*, *32*(1), 453–461.

Stalin, B., Nagaprasad, N., Vignesh, V., & Ravichandran, M. (2019). Evaluation of mechanical and thermal properties of tamarind seed filler reinforced vinyl ester composites. *Journal of Vinyl and Additive Technology*, *25*(s2), E114–E128.

Sutivisedsak, N., Cheng, H. N., Burks, C. S., Johnson, J. A., Siegel, J. P., Civerolo, E. L., & Biswas, A. (2012). Use of nutshells as fillers in polymer composites. *Journal of Polymers and the Environment*, *20*(2), 305–314.

Vaisakh, S. S., Peer Mohammed, A. A., Hassanzadeh, M., Tortorici, J. F., Metz, R., & Ananthakumar, S. (2016). Effect of nano-modified SiO_2/Al_2O_3 mixed-matrix micro-composite fillers on thermal, mechanical, and tribological properties of epoxy polymers. *Polymers for Advanced Technologies*, *27*(7), 905–914.

Vignesh, V., Balaji, A. N., & Karthikeyan, M. K. V. (2016). Extraction and characterization of new cellulosic fibers from Indian mallow stem: An exploratory investigation. *International Journal of Polymer Analysis and Characterization*, *21*(6), 504–512.

Vignesh, V., Balaji, A. N., & Karthikeyan, M. K. V. (2017). Effect of wood sawdust filler on the mechanical properties of Indian mallow fiber yarn mat reinforced with polyester composites. *International Journal of Polymer Analysis and Characterization*, *22*(7), 610-621.

Vigneshwaran, S., Uthayakumar, M., & Arumugaprabu, V. (2019). Development and sustainability of industrial waste-based red mud hybrid composites. *Journal of Cleaner Production*, *230*, 862–868.

Zheng, H., Sun, Z., & Zhang, H. (2019). Effects of walnut shell powders on the morphology and the thermal and mechanical properties of poly (lactic acid). *Journal of Thermoplastic Composite Materials*, *20*(10), 1-13.